X-Ray Micrography and Imaging of *Escherichia coli* Cell Shape Using Laser Plasma Pulsed Point X-Ray Sources

Jayshree M. Rajyaguru,* Masataka Kado,# Martin C. Richardson,# and Michael J. Muszynski*
*Department of Pediatric Infectious Diseases Research, Arnold Palmer Hospital for Children and Women, Orlando, Florida 32806, and #Center for Research and Education in Optics and Lasers, University of Central Florida, Orlando, Florida 32826-2700 USA

ABSTRACT High-resolution x-ray microscopy is a relatively new technique and is performed mostly at a few large synchrotron x-ray sources that use exposure times of seconds. We utilized a bench-top source of single-shot laser (ns) plasma to generate x-rays similar to synchrotron facilities. A 5 μl suspension of *Escherichia coli* ATCC 25922 in 0.9% phosphate buffered saline was placed on polymethylmethyacrylate coated photoresist, covered with a thin (100 nm) SiN window and positioned in a vacuum chamber close to the x-ray source. The emission spectrum was tuned for optimal absorption by carbon-rich material. Atomic force microscope scans provided a surface and topographical image of differential x-ray absorption corresponding to specimen properties. By using this technique we observed a distinct layer around whole cells, possibly representing the Gram-negative envelope, darker stained areas inside the cell corresponding to chromosomal DNA as seen by thin section electron microscopy, and dent(s) midway through one cell, and ⅓- and ⅔-lengths in another cell, possibly representing one or more division septa. This quick and high resolution with depth-of-field microscopy technique is unmatched to image live hydrated ultrastructure, and has much potential for application in the study of fragile biological specimens.

INTRODUCTION

Detection and study of microbial cells is performed by low-magnification optical microscopy and direct and indirect labeling techniques. In bacteriology, for resolution at 1–100-μm scale cationic (methylene blue, crystal violet, safranin) or anionic (eosin, acid fuchin, congo red) color dyes are used. In virology, for nanometer scale detection secondary-conjugated fluorescent markers such as antibodies are applied, and radioactively labeled substrate uptake is measured for very slow-growing Mycobacteria (Chapin-Robertson and Edberg, 1991). Visual ultrastructural studies on subcellular organelles are possible with variations of electron microscopy (thin section, scanning, and freeze fracture) although specimen preparation steps such as fixation, dehydration, resin embedding, ultra-thin sectioning, coating, and staining are very technical, extensive, and may introduce artifacts in the original sample. Although electron microscopy can be used at the nanometer resolution level, the sample preparation steps involved limit its use for routine studies of microbial cells (Kay, 1976; Lickfeld, 1976).

X-ray microscopy is a relatively new technique that has not been applied to any significant extent for biological specimens (DeMeis, 1996). X-ray microscopy eliminates the specimen preparation stages, which may alter the target, has resolution at the 100 Å level (Ohnesorge and Binning, 1993), and is able to probe the internal structures of in vitro assemblies to enable the observation of complex features in their natural, live state (Feder et al., 1985; Hoh and Hansma, 1992). Most x-ray microscope development has so far been made using large synchrotron sources (Neiman, 1992) and some with very large lasers (Ford et al., 1991). This has limited x-ray microscopy to a research tool mostly at major synchrotron facilities. The use of a laser plasma x-ray source simplifies the generation of the source x-rays, specimen handling, and overall ease of applicability for fragile biological specimens (Richardson et al., 1992; Shinohara, 1990). This idea was introduced earlier by Robbin Cotton (Cotton and Fletcher, 1992). The potential advantages of a laser plasma x-ray source stem from its compactness and flexibility. The spectral brightness of laser plasma x-ray sources is comparable to the brightest available synchrotron and can be generated under modest vacuum requirements. The x-ray emission spectrum of laser plasmas is rich in bright, broad (Planckian) continuum emission and in narrow atomic emission lines, and can be easily varied to suit specific microscopy needs. There is also selectivity in x-ray wavelengths to facilitate the elemental analysis of features within biological structures by difference imaging with emissions at two different wavelengths. Laser plasmas are point sources with high reproducibility and therefore fulfill the requirements of extremely high alignment specifications of precision x-ray optical systems.

Atomic force microscopy (AFM) is derived from the scanning tunneling microscope (Binning et al., 1982) and provides detailed topographic maps of sample surfaces (Tillmann et al., 1992). The AFM maps surfaces by raster-scanning a fine tip gently over the sample surface, resulting

Received for publication 11 November 1996 and in final form 31 December 1996.

Address reprint requests to Dr. Jayshree M. Rajyaguru, Department of Pediatric Infectious Diseases Research, Arnold Palmer Hospital for Children and Women, 85 West Miller Street, Suite 303, Orlando, FL 32806. Tel.: 407-649-9111 x5691; Fax: 407-426-7553; E-mail: 75301.3426@compuserve.com.

These data were presented as part of paper no. 4763 in the Imaging Slide Session at the Experimental Biology '96 Conference (FASEB), April 14–17, 1996, Washington DC.

0006-3495/97/04/1521/06 $2.00

in a 3-dimensional profile of the surface at a resolution that can be as high as atomic resolution on hard flat surfaces (Binning et al., 1987; Panessa-Warren and Warren, 1980). Several DNA-protein complexes have been imaged with an AFM including DNA-*E.coli* RNA polymerase (Hansma et al., 1993; Rees et al., 1993; Zenhausern et al., 1992), DNA polymerase (Yang et al., 1992), *Eco*RI restriction enzyme (Nui et al., 1993), and the large T-antigen of SV-40. Biological membranes containing phospholipid mono, bi, and multilayers (Zasadzinski et al., 1991), individual reconstituted proteins e.g., fibrinogen (Wigren et al., 1991), immunoglobulins (Hansma et al., 1991; Ill et al., 1993), phosphorylase kinase complexes (Edstrom et al., 1990), and α-macroglobulin (Arakawa et al., 1992) as well as protein arrays in lipid membranes, have also been investigated (Arnsdorf and Lal, 1992; Meyer-Ilse et al., 1992; Schabert et al., 1995) with the AFM. Scanning electron microscopy has been the method of choice for reading the x-ray-exposed resist until the AFM became available. Use of the AFM for reading the resist is the fastest method and also eliminates the prerequisite of metal coating the resist before an image can be obtained.

In collaboration with the Center for Research and Education in Optics and Lasers at the University of Central Florida (Orlando, FL) we performed a pilot study to test the ultramicrography technique described above to obtain high-resolution images of *E. coli*, other bacteria, and macromolecules (Kado et al., 1996; Rajyaguru et al., 1995; 1996a,b).

MATERIALS AND METHODS

Whole cells

An overnight culture of *E. coli* ATCC 25922 from sheep blood agar plate incubated at 35°C in 5% CO_2 was directly suspended at 10^8 cfu/ml in 0.9% phosphate buffered saline (PBS) pH 7.4 (Sigma, St. Louis, MO). A 5-μl drop of the suspension was streaked onto the PMMA-coated photoresist (Fastec Fabrications Ltd., Northants, UK) and covered with a SiN window (Fastec Fabrications Ltd., Northants, UK) before exposure to x-rays.

Exposure to x-rays

PMMA acts as a photographic film negative to absorb the x-ray absorption profile of the specimen placed on it. The dimensions of the photoresist and the window are both 5 mm × 5 mm. This photoresist was placed under vacuum at room temperature at a distance of 2.5 cm from a silicon target disk (Fig. 1). The silicon plasma produced by a 10-ns burst of laser energy at 20 J radiated strong emission lines in the region of 300 eV. The soft x-rays were generated as a pyramid of radiation with the target as the apex, 1–10 nm in wavelength, which pass through the specimen holder window. Since the target is ~25 mm away from the specimen, and the window in the specimen holder is 5 mm wide, there will be a variation in beam angle of ~11°. The intensity of x-rays that passed through the specimen and reached the surface of the photoresist was inversely proportional to the amount absorbed by the specimen. The difference in intensities was recorded on the photoresist as radiation damage. The resulting uneven structure on the photoresist was then scanned with an AFM.

Photoresist development

After exposure to x-rays, the photoresist was developed briefly by one wash (5 min) in sodium hypochlorite; two min wash in 4-methyl-2-pentanone to develop the image, and then rinsed in 2-propanol to stop overdevelopment of the image. The photoresist was then examined by an AFM to obtain a digital image of the absorption profile.

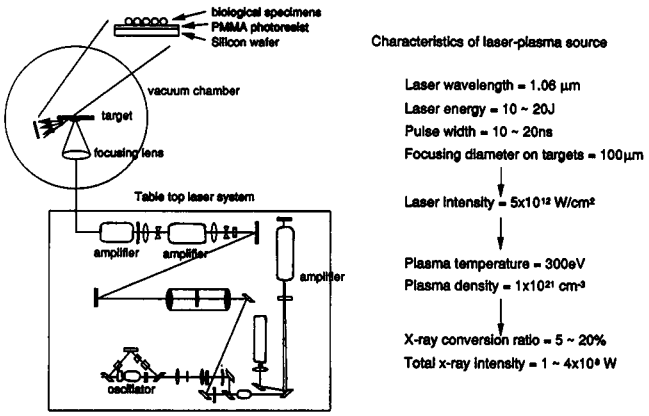

FIGURE 1 Laser plasma facility for x-ray microscopy.

Atomic force microscopy

A scanning probe microscope (TMX-2000; Topometrix, CA) was used with TMXSPM software. A 200-μm-long cantilever silicon nitride tip was used to obtain x-ray images from the developed photoresist.

RESULTS

The table top setup of the laser plasma x-ray generation system (Figs. 1 and 2) is significantly smaller and easier to handle in comparison with the expensive elaborate synchrotron x-ray generation systems used for this type of microscopy. The total time required from streaking the culture onto a plate to the final AFM image is 32 h. This 32-h time includes 24-h incubation of the plate, 2–3 laser shots (4 h), and up to five scans on the AFM of each x-ray-exposed resist (4 h) to confirm consistency of specimen and images. Figs. 3 and 4 show lower resolution (0–10 μm and 0–5 μm scale, respectively) images of cells of *E. coli* ATCC 25922. *E. coli* is well known as a Gram-negative straight rod-shaped bacterium. However, the images in Figs. 3 and 4 both show a slight bend to the rod shape of the bacterium. Also noticeable in both Figs. 3 and 4 is a nonuniformity in the density of cell composition. Topographical representation (Fig. 5) of Fig. 4 stresses the bend in the cell shape, and arrows point to the enhanced dents in the cells, which may correspond to division septa. Color representation of the topographical image in Fig. 5 greatly clarifies the overall bent shape of the cells, the positions of possible septa, and the distinct difference in the x-ray absorption by a layer around the cell, which may represent the highly organized Gram-negative cell envelope.

DISCUSSION

High-resolution imaging of fixed nonliving specimens is routinely performed in the field of materials science and

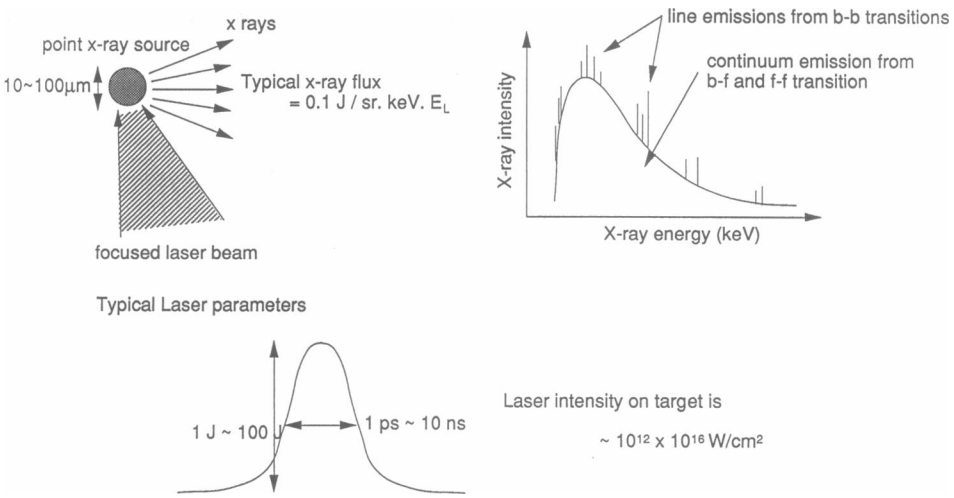

FIGURE 2 Pulsed point laser plasma sources.

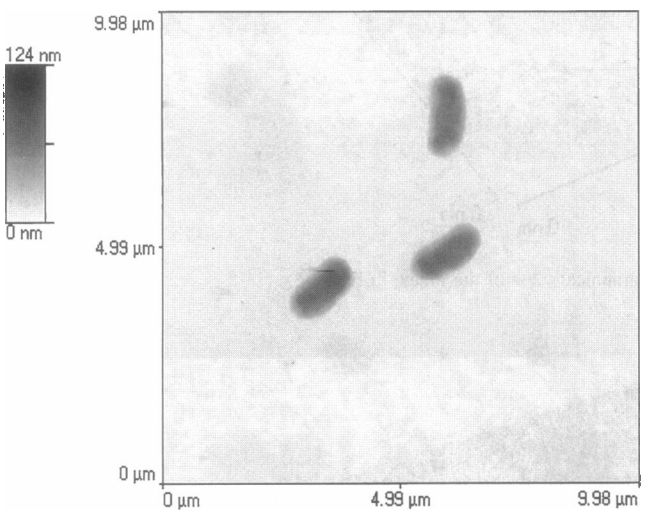

FIGURE 3 Low resolution AFM image of surface view of *E. coli* ATCC 25922 cells from x-ray-exposed photoresist.

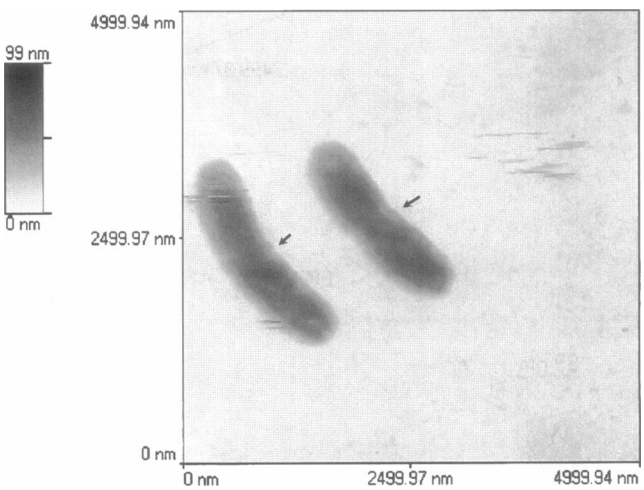

FIGURE 4 High-resolution AFM image of surface view of *E. coli* ATCC 25922 from x-ray-exposed photoresist. Arrow points to possible division septa in the cells.

optical physics under extremely clean and controlled conditions. However, in spite of the need for such technology, applications for analysis and study of biological specimens has predominantly been restricted to the various types of electron microscopy. The extensive specimen preparation and specialized handling of fixed, dehydrated cells or macromolecules is time-consuming, and therefore it is expensive, even though the materials required for this established technique are now relatively inexpensive. For a preliminary application of x-ray microscopy to a biological specimen, we chose *E. coli* as a unicellular, easy-to-handle prokaryotic cell, which has also been extensively studied by various other methods.

The images that we obtained are certainly different from what has been observed by other types of direct microscopy techniques, such as low-magnification optical, fluorescence, or high-magnification electron microscopy (EM). The reproducible slightly curved cell shape of the *E. coli* cells seen in Figs. 3–6, if true, contrasts the well-accepted notion that all Gram-positive and Gram-negative rod-shaped bacteria may not be straight rods after all. All the clearly visible dents in the cells (Figs. 4–6) clearly point to what is most likely to be the division septum, of which there may be more than one at a time as illustrated in Figs. 5 and 6. This also contradicts the idea that bacteria divide by elongation followed by separation at the middle, once the chromosomal material is duplicated and one copy is localized in each of the two daughter cells. Another feature seen in the x-ray micrographs (Figs. 4 and 6) is the consistent and distinct layer seen around the cell. Gram-negative bacteria are known to have a multilayered envelope different from Gram-positive bacteria, which is the basis of the Gram stain that differentiates the two categories of bacteria. It is very tempting to postulate that the layer seen around the *E. coli* cells, which strictly represents a difference in x-ray absorption as compared with the material next to it, i.e., the mixed-up cytoplasmic constituents inside the cell, is the envelope. As seen by thin-section electron microscopy, this

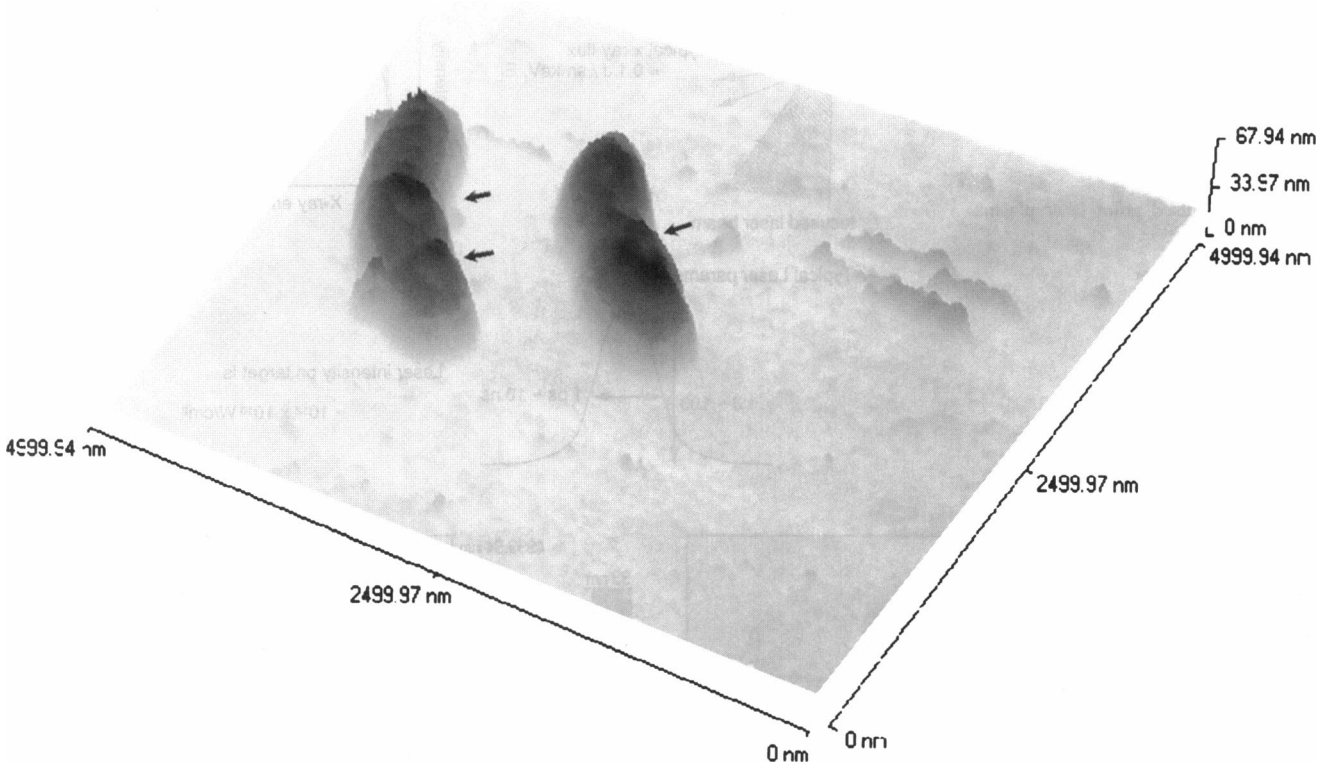

FIGURE 5 AFM image showing the topographical view of the image in Fig. 2.

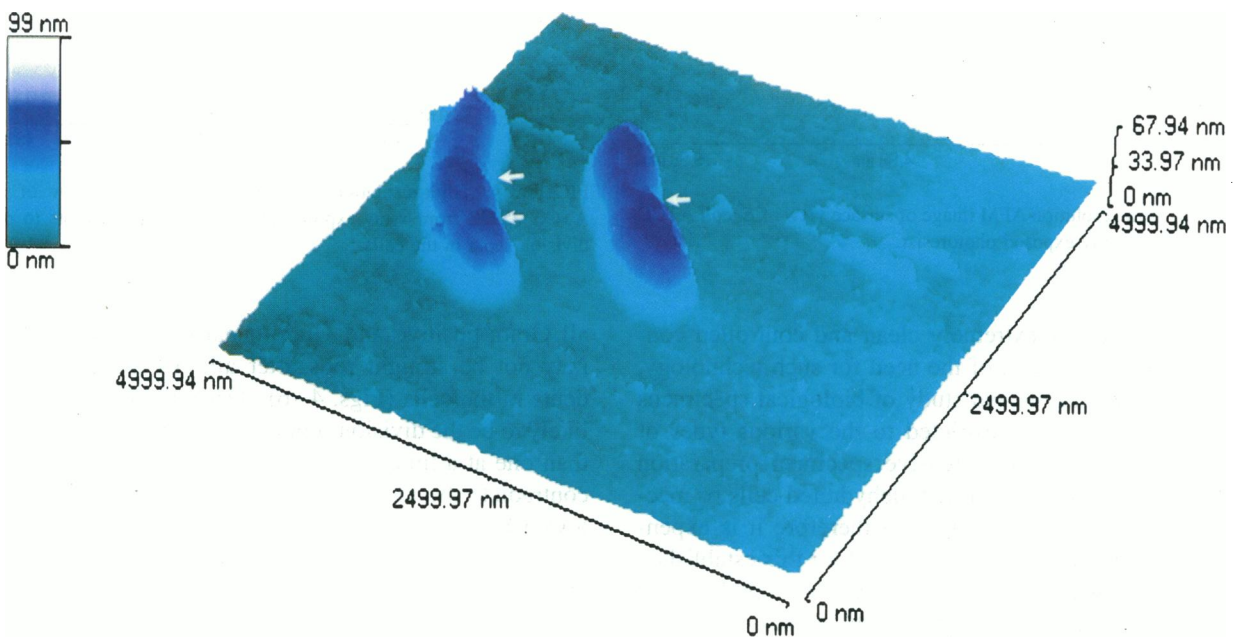

FIGURE 6 Color image of the topographical view of image in Fig. 2.

envelope is present consistently around the cell and is also composed of at least four sublayers, the asymmetric lipopolysaccharide and phospholipid layers of the outer membrane, the thin peptidoglycan layer, and the cytoplasmic membrane, respectively; however, we do not see any sublayers in these images (Figs. 3–6).

The combination of x-rays generated from laser-produced plasma and scanning probe microscope to scan images is ideal for examination of microbial cells and macromolecules. This technique eliminates the sample preparation steps for microscopic analysis. No color dyes, conjugated fluorescent antibodies, or radioactive labels are necessary

due to the high resolution of the scanning probe microscope. The short (10 ns) exposure to x-rays is too short to introduce dehydration, physical sample degradation, plasmolysis for whole cells, or enzymatic degradation of cell constituents; thus, the absorption profile of the specimen would be unaltered by this technique. The x-ray image on the PMMA-coated resist is permanent and can be examined in contact or noncontact mode with the scanning probe microscope. For large samples, e.g., *Candida albicans*, and other eukaryotic cells in the 5–100 μm range, a larger tip size can be used to produce a whole cell image, in combination with a fine tip to scan the same image at nanometer resolution. The x-rays are certainly strong enough to damage the specimen, and with the present system we would be unable to retrieve enough of irradiated specimen under sterile conditions to start a culture, and hence we have not studied any postexposure effects on the organism. However, we speculate a higher mutation rate in the irradiated cells due to damage to the nucleic acids, similar to UV damage.

Laser-produced plasma x-ray and scanning probe microscopy is unmatched in its efficiency, cost, resolution, depth of field, minimal sample preparation and handling, permanent image record, dimensional detail, computer-assisted color coding, and ease of applicability to the study of biological specimens, especially microbial cells and their macromolecules (Table 1). X-ray microscopy as studied in this brief report suggests a new and exciting field that requires the establishment of a library of reference images to serve as baseline for further, more complex-interaction visual studies at the molecular level. There is great potential to discover new natural features in hydrated cells and molecules directly in their dynamic state due to minimal sample handling, treatment, and labeling requirements. Implications for the direct visual study of new and existing drug interaction with target sites such as enzyme inhibition by competition, receptor blockage, and receptor stimulation in various disease states are outstanding. The relatively short period of time (30 min) required to obtain high-resolution images from natural hydrated samples simplifies the study of a large number of samples of a variety of fungi, protozoa, bacteria, and viruses, specimens of which need not be present in large numbers. Heavy metal or latex microsphere conjugated monoclonal antibodies can also be used to localize specific markers in the cell.

TABLE 1 Comparison of microscopies

Microscope	Wavelength (nm)	Numerical Aperture	Resolution (nm)	Depth of Field (nm)
Optical	500	0.7	435	1244
		1.4	218	311
X-Ray	3.2	0.02	90	8200
	2.5	0.6	20	520
STEM*	100 kV	0.005	0.5	0.37

*Scanning transmission electron microscopy.

Lastly, pulsed laser plasmas introduce the time domain element into x-ray microscopy. Exposure times for microscopy with synchrotrons are measured in seconds; the laser plasmas utilized here can provide x-ray emission in pulses ranging from several nanoseconds to 1 picosecond. This introduces the possibility of capturing kinetic, chemical, or morphological snapshots of biological ultrastructures in time frames of interest to understanding complex biological processes. No other type of microscopy offers this potential.

This work was supported by the Orlando Regional HealthCare Foundation, the State of Florida, and the Air Force Office of Scientific Research.

REFERENCES

Arakawa, H., K. Umemura, and A. Ikai. 1992. Protein images obtained by STM, AFM and TEM. *Nature.* 358:171–173.

Arnsdorf, M. F., and R. Lal. 1992. Recent progress with atomic force microscopy in biology: molecular resolution of cell membranes, constituent biomolecules, and microcrystals. *SPIE (Imaging Technologies and Applications).* 1778:112–116.

Binnig, G., C. Gerber, E. Stoll, R. T. Albrecht, and C. F. Quate. 1987. Atomic resolution with atomic force microscope. *Europhys. Lett.* 3:1281–1286.

Binnig, G., H. Rohrer, C. Gerber, and E. Weibel. 1982. Surface studies by scanning tunneling microscopy. *Phys. Rev. Lett.* 49:57–61.

Chapin-Robertson, K., and S. C. Edberg. 1991. *In* Manual of Clinical Microbiology. 5th ed, Chap. 4. A. Ballows, W. J. Hausler, Jr., K. L. Herrman, H. D. Isenberg, and H. J. Shadomy, editors. American Society for Microbiology, Washington DC. 29–35.

Cotton, R. A., and J. Fletcher. 1992. Bringing soft x-ray contact microscopy to the biologist. *Proc. RMS.* 27:77–80.

DeMeis, R. 1996. X-ray imaging. Laser plasma "x-rays" living organsims. *Laser Focus World.* June: 37–38.

Edstrom, R. D., M. H. Meinke, X. R. Yang, R. Yang, V. Elings, and D. F. Evans. 1990. Direct visualization of phosphorylase-kinase complexes by scanning tunneling and atomic force microscopy. *Biophys. J.* 58: 1437–1448.

Feder, R., V. Banton, D. Sayre, J. Costa, M. Baldini, and B. Kim. 1985. Direct imaging of live human platelets by flash X-ray microscopy. *Science.* 227:63–64.

Ford, T. W., A. D. Stead, and R. A. Cotton. 1991. Soft x-ray microscopy of biological materials. *Electron Microsc. Rev.* 4:269–292.

Hansma, H. G., M. Bezanilla, F. Zenhausern, M. Adrian, and R. L. Sinsheimer. 1993. Atomic force microscopy of DNA in aqueous solutions. *Nucleic Acids Res.* 21:505–512.

Hansma, H. G., A. L. Weisenhorn, A. B. Edmundson, H. E. Gaub, and P. K. Hansma. 1991. Atomic force microscopy: seeing molecules of lipid and immunoglobulin. *Clin. Chem.* 37:1497–1501.

Hoh, J. H., and P. K. Hansma. 1992. Atomic force microscopy for high resolution imaging in cell biology. *Trends Cell Biol.* 7:208–213.

Ill, C. R., V. M. Keivens, J. E. Hale, K. K. Nakamura, R. A. Jue, S. Cheng, E. D. Melcher, B. Drake, and M. C. Smith. 1993. A COOH-terminal peptide confers regiospecific orientation and facilitates atomic force microscopy of an IgG/sub 1. *Biophys. J.* 64:919–924.

Kado, M., K. Nekula, M. C. Richardson, Y. Yamamoto, and H. Friedman. 1996. Direct ultrastructural imaging of macrophages using a novel X-ray contact microscopy (Abstr. 4762). *In* Abstracts of the Experimental Biology Conference 96, Washington, DC. *FASEB J.* 10:824.

Kay, D. 1976. Electron microscopy of small particles, macromolecular structures, and nucleic acids. *In* Methods in Microbiology—1976, Vol. 9. J. R. Norris, editor. Academic Press, London. 177–215.

Lickfeld, K. G. 1976. Transmission electron microscopy of bacteria. *In* Methods in Microbiology—1976, Vol. 9. J. R. Norris, editor. Academic Press, London. 127–176.

Meyer-Ilse, W., P. A. Gutmann, J. Thieme, D. Rudolph, G. Schmahl, E. Anderson, P. Batson, D. Attwood, N. Isklander, and D. Kern. 1992. Experimental characterization of zone plates for high resolution. *In* X-ray Microscopy III. A. G. Michette, G. R. Morrison, and C. J. Buckley, editors. Springer Verlag, Berlin. 284–289.

Neiman, B. 1992. X-ray microscope with the Gottingen scanning X-ray microscope at 2.4 nm. *In* X-ray Microscopy III. A. G. Michette, G. R. Morrison, and C. J. Buckley, editors. Springer Verlag, Berlin. 143–150.

Nui, L., W-L. Shaiu, J. Vesenka, D. D. Larson, and E. Henderson. 1993. Atomic force microscopy of DNA-colloidal gold and DNA-protein interactions. *SPIE.* 1891:71–77.

Ohnesorge, F., and G. Binning. 1993. True atomic resolution by atomic force microscopy through repulsive and attractive forces. *Science.* 260: 1451–1456.

Panessa-Warren, B. J., and J. B. Warren. 1980. Determining biological fine structure by differential absorption of soft x-rays. *Ann. NY Acad. Sci.* 342:350–367.

Rajyaguru, J. M., M. J. Muszynski, M. Kado, and M. Richardson. 1995. Application of x-rays to obtain ultrastructural images of microbes and macromolecules (Abstr. J-9). *In* Abstracts of the 95th General Meeting of the American Society for Microbiology. Washington, DC. p. 535.

Rajyaguru, J. M., M. Kado, K. Nekula, D. Torres, M. Richardson, and M. J. Muszynski. 1996a. Direct high resolution (nm scale) ultrastructural X-ray imaging of live hydrated *Escherichia coli* (Abstr. J-7). *In* Abstracts of the 96th General Meeting of the American Society for Microbiology. Washington, DC. p. 473.

Rajyaguru, J. M., M. Kado, K. Nekula, D. Torres, M. Richardson, and M. J. Muszynski. 1996b. Ultrastructural X-ray imaging and molecular modelling of hydrated biological specimen using laser plasma pulsed point X-ray sources (Abstr. 4763). *In* Abstracts of the Experimental Biology Conference 96, Washington, DC. *FASEB J.* 10:A824.

Rees, W. A., R. W. Keller, J. P. Vesenka, C. Yang, and C. Bustamante. 1993. Scanning force microscopy imaging of transcription complexes: evidence for DNA bending in open promoter and elongation complexes. *Science.* 260:1646–1649.

Richardson, M., K. Shinohara, K. A. Tanaka, Y. Kinjo, N. Ikeda, and M. Kado. 1992. Pulsed X-ray microscopy of biological specimen with laser plasma sources. *SPIE Soft X-ray Microscopy.* 1741:133–141.

Schabert, F. A., C. Henn, and A. Engel. 1995. Native *Escherichia coli* OmpF porin surfaces probed by atomic force microscopy. *Science.* 268:92–94.

Shinohara, K. 1990. Application of X-ray microscopy to mammalian cells. *In* X-ray Microscopy in Biology and Medicine. K. Shinohara, K. Yada, H. Kihara, and T. Saito, editors. Springer Verlag, Berlin. 203–212.

Tillmann, R., M. Radmacher, and H. E. Gaub. 1992. Hydrated amorphous silicon oxide surface at 3 angstrom resolution by scanning force microscopy. *Appl. Phys. Lett.* 60:3111–3113.

Wigren, R., H. Elwing, R. Erlandson, S. Welin, and I. Lundstrom. 1991. Structure of fibrinogen obtained by scanning force microscopy. *FEBS Lett.* 280:225–228.

Yang, J., K. Takeyasu, and Z. Shao. 1992. Atomic force microscopy of DNA molecules. *FEBS Lett.* 301:173–176.

Zasadzinski, J. A., C. A. Helm, M. L. Longo, A. L. Weisenhorn, S. A. Gould, and P. K. Hansma. 1991. Atomic force microscopy of hydrated phosphatidyl-ethanolamine bilayers. *Biophys. J.* 59:755–760.

Zenhausern, F., M. Adrian, Bt. Heggeler-Bordier, L. M. Eng, and P. Descouts. 1992. DNA and RNA polymerase/DNA complexes images by scanning force microscopy: influence of molecular-scale friction. *Scanning.* 14:212–217.